

Influence of Parallelism in Vector-Multiplication Units on Correlation Power Analysis

Manuel Brosch, Matthias Probst, Stefan Kögler, Georg Sigl

Abstract—The use of neural networks in edge devices is increasing, which introduces new security challenges related to the neural networks’ confidentiality. As edge devices often offer physical access, attacks targeting the hardware, such as side-channel analysis, must be considered. To enhance the performance of neural network inference, hardware accelerators are commonly employed. This work investigates the influence of parallel processing within such accelerators on correlation-based side-channel attacks that exploit power consumption. The focus is on neurons that are part of the same fully-connected layer, which run parallel and simultaneously process the same input value. The theoretical impact of concurrent multiply-and-accumulate operations on overall power consumption is evaluated, as well as the success rate of correlation power analysis. Based on the observed behavior, equations are derived that describe how the correlation decreases with increasing levels of parallelism. The applicability of these equations is validated using a vector-multiplication unit implemented on an FPGA.

Index Terms—side-channel analysis, correlation power analysis, vector-multiplication, neural networks

I. INTRODUCTION

In an increasing number of applications, Artificial Intelligence (AI) is utilized in the form of Neural Networks (NNs), which are also used on often resource-constrained edge devices to perform complex tasks, such as image recognition. Edge AI reduces the latency since the device must not send data to a larger instance to perform the classification there. Hence, the bandwidth requirements are lower compared to a classical cloud-based AI application. Another benefit is that the data is kept private on the device. However, edge AI is primarily limited to the inference of NNs. Nevertheless, already the execution of a trained NN on a resource-constrained device is challenging. Optimization techniques like pruning and quantization are used to reduce the amount of operations and their complexity [1]–[3]. Through the mentioned methods a performant execution of NNs with limited resources is enabled [4]. In addition, dedicated hardware accelerators enhance the parallelism and minimize latency.

But edge AI also harbors new risks that threaten the confidentiality of a trained NN. Attacks that target hardware weaknesses of an implementation must be considered, as an adversary can gain physical access to an edge device that

Manuel Brosch, Matthias Probst and Stefan Kögler are with the TUM School of Computation, Information and Technology, Chair of Security in Information Technology, Technical University of Munich, 80333 Munich, Germany (e-mail: manuel.brosch@tum.de; matthias.probst@tum.de).

Georg Sigl is with the TUM School of Computation, Information and Technology, Chair of Security in Information Technology, Technical University of Munich, 80333 Munich, Germany, and also with the Fraunhofer Institute for Applied and Integrated Security, 85748 Garching, Germany.

executes an NN. Side-Channel Analysis (SCA) is a prominent example, which exploits information leakage through physical quantities such as time, power consumption, or Electro-Magnetic (EM) emanations. A widespread side-channel attack is Correlation Power Analysis (CPA), which uses the power consumption of a device in combination with statistical methods to extract valuable information [5]. Techniques like CPA are predominantly used in the cryptographic area but can also be used to retrieve information about an unknown NN being executed on a device. As training an NN is complex and costly, extracting it can be a worthwhile goal to steal the intellectual property in the form of the NN.

Different implementations have already been analyzed and allow the extraction of the architecture as well as the weight and bias parameters from pure side-channel information, cf. [6], [7]. However, state-of-the-art side-channel attacks aiming to extract an NN focus predominantly on sequential or non-highly parallelized implementations. The research conducted by Gongye et al. [8] concentrates on a strongly parallelized accelerator, demonstrating that parameter extraction using SCA is feasible only in a simplified corner case. The authors, though, do not analyze the effects of parallel calculations on the quality of measurable side-channel information and the impact on Signal-to-Noise Ratio (SNR).

Current research indicates that global side-channel information, such as power consumption or overall EM emissions, cannot be effectively used to extract parameters of unknown NNs running on highly parallel accelerators. Instead, localized EM measurements are necessary to minimize the impact of other calculations occurring simultaneously. However, a formal and detailed analysis of how parallel vector multiplications in AI accelerators affect the success of correlation-based SCA has not yet been conducted.

This work contributes to the literature by demonstrating how parallelism influences the success rate of CPA. Additionally, it evaluates the temporal component, specifically how the number of calculations already performed affects the performance of a SCA. The focus is on concurrently processed neurons that are used in fully-connected layers of NNs such as Multi-Layer Perceptrons (MLPs) or Convolutional Neural Networks (CNNs). Neurons within the same layer process the identical input value simultaneously but with an individual weight value, which leads to a statistical dependency of the intermediate results. An adversary seeks to retrieve the weights of the neurons by CPA using the overall power consumption or global EM emanation of the device. The architecture is not considered in this work as publications show that an adversary

can also extract the architecture from parallel implementations, cf. [8]. This work aims to determine the maximum number of parallel operating neurons for which a CPA-based weight retrieval remains feasible. In addition, a boundary is determined from which onwards parallelism hinders a power-based CPA and localized EM measurements are required to extract information about the parameters of the NN. The main contributions are:

- 1) This work provides a theoretical behavioral description of the power consumption of a vector-multiplication unit and analyzes how parallel data processing affects it.
- 2) The influence of parallel-processed neurons in a fully-connected layer on CPA attacks aiming to extract the individual neuron weights is examined. Equations are derived that describe the reduction in the correlation coefficient for the correct weight hypothesis as a function of the degree of parallelism.
- 3) The validity of the theoretical findings is demonstrated through practical measurements of a vector-multiplication unit implemented on a Field Programmable Gate Array (FPGA), where the degree of parallel multiplications can be freely adjusted.

A. Related Work

Several works demonstrate that SCA represents a serious threat to NNs in the form of model stealing attacks. Focusing on software and sequential implementations, Batina et al. show that with EM measurements an unknown NN can be fully reverse engineered [6]. They use CPA to extract weights and bias values. The architecture is extracted by utilizing Simple Power Analysis (SPA) in combination with CPA. The timing of the function is used as a distinguisher to determine the implemented activation function. Hence, some profiling is necessary to template the timings of different activations. Takatoi et al. improve the work of Batina et al. by extracting the type of activation from EM side-channel information as well [9]. Besides the EM side-channel, Maji et al. show that the power side-channel can be used to retrieve NNs from several microcontrollers [10]. They use SPA and the timing to fully extract an NN.

Several works also evaluate the side-channel characteristics of dedicated AI accelerators. Yu et al. target a so-called Binarized Neural Network (BNN) that is implemented on an FPGA [11]. They exploit EM information to reveal the architecture of the network. Subsequently, they use the extracted architecture in combination with adversarial active learning to estimate the parameters of the NN. However, their attack requires the complete classification results of the implemented network and not just the label, which is predicted by the network for a given input. Additionally, their results show that estimating the parameters leads to deviations in the accuracy of the NN. Yoshida et al. demonstrate an attack on an FPGA that implements a systolic array to extract the processed weights [7]. The accelerator implements interconnected Processing Elements (PEs) that operate in a pipelined fashion. The authors analyze a 3×3 PE array where each PE performs a

Multiply-and-Accumulate (MAC) operation. By measuring the power consumption and performing several CPAs sequentially, the noise within the measurements is reduced, allowing the extraction of the parallelly processed weights. A highly parallel accelerator is targeted in [8]. Similar to other work, they use EM traces to reveal the unknown NN architecture. The authors also demonstrate the extraction of weight parameters of kernels in the first two layers. However, the kernel parameter retrieval only works for filters with one input and output channel. A kernel with two channels is already more complicated to attack due to the parallel processing, as mentioned by the authors. Hence, the attacker must either adapt the hypotheses to include all weights processed at a time or a local EM probe is required to measure individual PEs.

II. BACKGROUND

This section provides fundamentals to CPA and NNs. Also, the assumed threat model is defined.

A. Correlation Power Analysis

Correlation Power Analysis (CPA) is a differential attack that utilizes statistical methods to exploit data dependencies in a physical quantity such as the power consumption [5]. The goal is to extract secret information. CPA is used in the field of classical NNs to retrieve weight and bias values of neurons in software [12] and hardware implementations [7]. For an effective CPA, a target operation must be chosen to combine known data with the secret data an adversary wants to retrieve. For NNs, the multiplication of the known input and the secret weights is typically selected, cf. [7], [12]. The attacker needs to record the device's power consumption or EM emanations while varying input data is processed. With the different known inputs and assumptions on the weights, the attacker builds up hypothetical intermediate results. These intermediate results are transferred to theoretical power values with the help of a so-called power model. Typical examples are the Hamming Weight (HW) or Hamming Distance (HD) power model, which assume that the power consumption is proportional to the number of bits set in a value or the number of bit-changes between two consecutive values. Pearson's correlation coefficient between the hypothetical and measured power values is calculated to identify the correct weight candidate in the targeted implementation. The highest absolute correlation coefficient yields the correct weight. More detailed information can be found in [7], [12].

B. Neural Networks

Neural Networks (NNs) allow the approximation of any function and perform classifications based on various parameters. The approximation is achieved by letting an NN undergo an iterative learning process, where the network parameters are determined. The NN learns the mapping between input vectors and the corresponding output class within a training set. Thereby, the network parameters are updated until the classification error of the training set is at a (local) minimum. After training, the NN can classify unknown inputs.

Basic building blocks of NNs are interconnected neurons, where the dot product of an input vector \mathbf{x} and the neuron weight vector \mathbf{w} is calculated according to

$$o = \phi \left(\sum_{i=0}^{N-1} (x_i \cdot w_i) + b \right). \quad (1)$$

The bias value b is added to the final product, as shown in Eq. (1). The result is fed into a non-linear activation function $\phi(\cdot)$, where functions like Rectified Linear Unit (ReLU) or Sigmoid are typical examples. Feed-forward NNs use several artificial neurons organized in layers. The input vector propagates through the layers and their respective neurons until the last layer provides the classification result. So-called MLPs feature layers only consisting of neurons according to Eq. (1), which are called fully-connected layers. CNNs additionally employ convolutional layers that perform a discrete convolution between the input and a kernel [13].

C. Threat Model

A passive attacker is assumed with physical access to the device, similar to the works [7], [12], [14]–[18]. The attacker aims to extract the NN from the device and obtain an identical clone of the implemented network. With that, the adversary can craft powerful adversarial examples [19] or leak information about training data, which results in a privacy breach [20], for instance. To reveal the parameters of the NN, the attacker can observe the device during its regular operation and may apply chosen inputs to the NN. However, the adversary cannot tamper with it. Consequently, active attacks such as fault injections are not considered in this work. Further, a pre-trained NN is assumed, where the adversary does not influence the training process, and the model is securely deployed on the accelerator, where the attacker cannot simply dump the memory. In summary, the adversary has no information about the executed NN, i.e., the architecture and parameters are unknown. The presented attack aims to exploit the physical access and the power consumption or global EM emanation side-channel to copy the network from the device. Advanced side-channel attacks that utilize localized EM emanations and may require an unpackaged device are out of scope of this work.

III. INFLUENCE OF PARALLEL VECTOR-MULTIPLICATION ON POWER ANALYSIS

The key operation to execute an NN is the multiplication of the weights with the corresponding inputs, cf. Eq. (1). In implementations, the vector-multiplication is accomplished by several so-called Multiply-and-Accumulate (MAC) operations. AI accelerators commonly implement an array of PEs, which performs the MAC operations. An example of such a realization is shown in Fig. 1, where each of the PEs processes a single neuron of the same fully-connected layer, i.e., the vector product between the individual weight vector \mathbf{w} of a neuron and the input vector \mathbf{x} is calculated. The input vector \mathbf{x} is connected to every PE because the input is the same for all neurons within a layer. Hence, at a specific point in time,

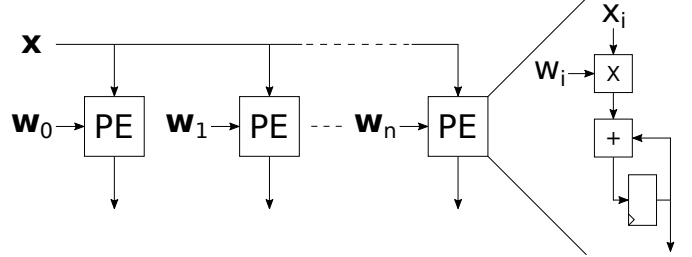


Figure 1: Hardware implementation of a vector-multiplication.

each PE processes the same input value but with a distinct weight. Taking a closer look at a PE reveals that it consists of a multiplier that calculates the product between a weight and an input value. The subsequent adder is used to sum up the product with the previous result, which is stored in the register. Consequently, a PE shown in Fig. 1 can perform one MAC operation in a single clock cycle.

The described PE array is a straightforward implementation of the vector-multiplication. More sophisticated AI accelerators use larger arrays of PEs in combination with techniques like systolic data processing to increase performance. However, the principle PE architecture remains the same also for different implementations. The focus is on the architecture shown in Fig. 1 to reduce the complexity of a power analysis attack. From an attacker's perspective, life is easier since just a single value of the input vector \mathbf{x} is processed at a time and not multiple inputs, which would increase the noise in the measurements.

The method of constructing individual PEs and integrating them into a vector-multiplication unit has likewise been adopted in prior studies [21]–[23]. The referred designs can either be adapted in the number of used PEs or are fixed to a defined amount. Moreover, in the work of Adiono et al. [24], a systolic array with nine PEs is proposed that processes the same input with nine different weights at a point in time, similar to the design shown in Fig. 1. Hence, the following results can be transferred to similar implementations.

In this context, the weights and input values processed by the PEs are limited to eight-bit integer values, i.e., a quantized NN is implemented. Using integers is a reasonable assumption on edge devices since quantized NNs are easier to process on devices with limited resources. The registers to store the intermediate results have a width of 32-bits. The limitations of the bit-sizes of the weights and inputs only affect the size of the hypotheses, but not the success of a CPA nor the effects of parallel processing. Consequently, the following findings remain valid also for different bit-widths of the weights and inputs.

For the subsequent simulation results, both weights and inputs are chosen uniformly random. Specifically, the weights are initialized with uniform random values at the beginning of a simulation run and remain constant throughout the run. During the simulation run, several power traces are generated, where the applied inputs for each trace are chosen randomly.

Consequently, the analysis does not rely on a real fully-connected layer of a trained NN. Nevertheless, this limitation does not affect the validity of the results or the success rate of the CPA, as the attack is independent of the specific values being processed.

A. Modeling the Power Consumption

The power consumption of an implementation depends on several components. Typically, the total power consumption P_{total} consists of a data-dependent component P_{data} , an operation dependent portion P_{op} as well as a constant and noise part, P_{const} and P_{noise} respectively [25]. Therefore, the power consumption is summarized to

$$P_{\text{total}} = P_{\text{data}} + P_{\text{op}} + P_{\text{const}} + P_{\text{noise}}. \quad (2)$$

For the theoretical analysis of how parallel processing of PEs influences power analysis attacks, P_{total} is simplified. It is assumed that the constant and noise components are zero. The constant power consumption can be eliminated in real-world measurements by adjusting the DC offset. The noise depends on the environment and is typically normally distributed [25]. Therefore, the noise can be reduced by calculating the mean of traces, where the same data is used. Consequently, due to the idealization, the power consumption depends only on the processed data and the performed operation. The assumptions result in the best-case scenario for power analysis attacks since they lead to the maximum SNR an adversary can achieve. For power analysis attacks, a combination of P_{op} and P_{data} is usually used, as a specific operation in combination with partially known data is targeted. Thus, the exploitable part of the power consumption P_{exp} consists of portions of P_{op} and P_{data} . Hence, the idealized power consumption equals

$$\hat{P}_{\text{total}} = P_{\text{exp}} + P_{\text{alg.noise}}, \quad (3)$$

where $P_{\text{alg.noise}}$ summarizes the unused parts of P_{op} and P_{data} .

Regarding the used implementation, the focus is on storing intermediate results in the register within a PE. The power consumed by the other components of a PE is neglected. Consequently, P_{exp} relates to the power consumed when storing a MAC result in the register of a single PE, while $P_{\text{alg.noise}}$ represents the power consumed by all other PEs that store their results in their registers. To model the power consumption of a PE, the commonly utilized HW and HD power models are employed. For the first multiplication at time $\tau = 0$, the HW model is used since the register is initialized to zero to ensure a correct vector product at the end. The power consumption of the subsequent MAC operations (i.e., $\tau > 0$) is modeled by the HD model since the register already holds a value, which is replaced by another. The following equations summarize how the power consumption of a PE is modeled:

$$\begin{aligned} z_{-1} &= 0 \\ z_\tau &= w_\tau \cdot x_\tau + z_{\tau-1} \\ P_{\text{PE},\tau} &= \text{HW}(z_\tau), \text{ at } \tau = 0 \\ P_{\text{PE},\tau} &= \text{HD}(z_{\tau-1}, z_\tau) = \text{HW}(z_{\tau-1} \oplus z_\tau), \text{ at } \tau > 0. \end{aligned} \quad (4)$$

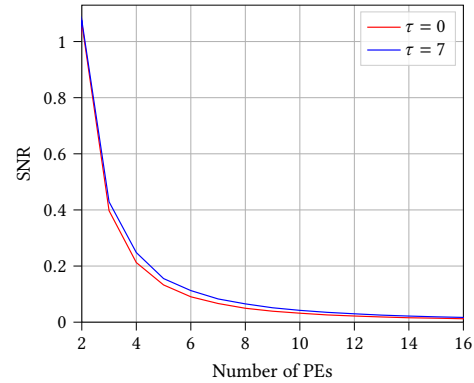


Figure 2: Theoretical SNR decrease of a single PE if other PEs operate in parallel. The SNR converges against zero when more than 16 PEs operate in parallel. 10,000 simulations are used for each number of PEs to calculate the averaged SNR.

The idealized total power consumption $\hat{P}_{\text{total},\tau}$ of the complete PE array at time τ , is the sum of the individual $P_{\text{PE},\tau}$.

B. Correlation Power Analysis

The success of a power analysis attack depends on the SNR of the measurements. The SNR is defined as the ratio between the variances of the exploitable power consumption and the noise [25]. For the idealized power consumption, the SNR is specified as

$$\text{SNR} = \frac{\text{Var}(P_{\text{exp}})}{\text{Var}(P_{\text{alg.noise}})}. \quad (5)$$

The SNR is depicted in Fig. 2 when modeling the power consumption of the PE array as described in Section III-A for 10,000 simulation runs with randomly chosen weight and input values. For P_{exp} , the power consumption of a single PE is used, while $P_{\text{alg.noise}}$ combines the sum of the power consumption portions of all other PEs in the array. As shown in Fig. 2, the SNR decreases in the same manner if more PEs are implemented independently of the point in time τ , which reflects the number of MAC operations that have been performed by each PE. In Fig. 2, the first result at $\tau = 0$ is shown, leaking the HW. Additionally, $\tau = 7$ is targeted, where already seven additions are stored, and the respective register changes its value from the seventh result to the eighth.

The behavior in Fig. 2 demonstrates that a power analysis becomes more challenging with an increasing number of PEs, i.e., parallel operations, which are not subject to the attack. However, methods like CPA are shown to be robust against noise and are often successful even for small SNR values [7]. To evaluate the effectiveness of a CPA, it is assumed that an adversary wants to extract the weights processed by a specific PE and other parallel running PEs process different weights. This assumption is reasonable since an attacker needs to build hypotheses on the secret weights and needs to compare all hypotheses with the measured power consumption. Therefore, the attacker is limited to a feasible number of hypotheses and cannot model the power consumption of all parallel operating

PEs. The hypothetical power consumption of the targeted PE or the correct weight hypothesis that is processed by this PE at time τ is denoted by $H_{\text{cw},\tau}$. The same power model is used to generate the hypotheses and the power traces. Therefore, the correct weight hypothesis $H_{\text{cw},\tau}$ achieves a correlation coefficient of one when just a single PE is implemented. The correlation coefficient ρ_τ for the correct weight hypothesis $H_{\text{cw},\tau}$ and the total power consumption $\hat{P}_{\text{total},\tau}$ can be calculated as

$$\rho_\tau = \frac{\mathbb{E} \left(H_{\text{cw},\tau} \cdot \hat{P}_{\text{total},\tau} \right) - \mathbb{E} (H_{\text{cw},\tau}) \cdot \mathbb{E} (\hat{P}_{\text{total},\tau})}{\sqrt{\text{Var} (H_{\text{cw},\tau}) \cdot \text{Var} (\hat{P}_{\text{total},\tau})}}, \quad (6)$$

where $\mathbb{E}(\cdot)$ denotes the expected value and $\text{Var}(\cdot)$ the variance. A simplification of Eq. (6) is possible if $H_{\text{cw},\tau}$ is statistically independent of the power consumption of all other PEs. For parallel operating implementations of cryptographic algorithms, the power consumption of simultaneously running components is usually statistically independent of each other because different inputs are processed in parallel. Therefore, the equations provided by Mangard et al. [25] are amendable. However, this is not the case for the assumed vector-multiplication unit, as the power consumption of each PE depends on an unknown weight and the current input value. As the input value is the same for all PEs, there is a statistical dependency between the power consumption values for different PEs.

The correlation between $H_{\text{cw},\tau}$ and the power consumption values of different PEs can confirm the mentioned dependency. If they are statistically independent, they should have a zero correlation. Figure 3 demonstrates the course of the correlation between $H_{\text{cw},\tau}$ and another P_{PE} , for random weight and input values as well as different points in time τ . For $\tau = 0$, i.e., when using the HW, the maximum correlation coefficient ρ_τ equals one. Hence, there is a directly linear relationship between $H_{\text{cw},\tau}$ and the power consumed by other PEs. The reason is that the intermediate results for different PEs are shifted linearly by different weight values. Consequently, the resulting theoretical power consumption values calculated by the HW of the intermediate results are just linear combinations of each other and, therefore, not statistically independent. Thus, the first multiplication result is not a suitable target for an attack since the weight values cannot be distinguished by CPA when multiple PEs are implemented. For later intermediate results, the maximum correlation between $H_{\text{cw},\tau}$ and other P_{PE} is smaller and stagnates for $\tau \geq 8$. The smaller correlation is due to more significant differences in the intermediate results that lead to dissimilar HD values. However, the variation in HD values is also limited. Thus, the decrease of ρ_τ stagnates from the point on, where the possible variation reaches its maximum.

The findings suggest that an attack targeting a later MAC operation is more successful since the hypotheses are more disjoint. However, aiming a later MAC calculation requires the consideration of more weights in the hypotheses. For

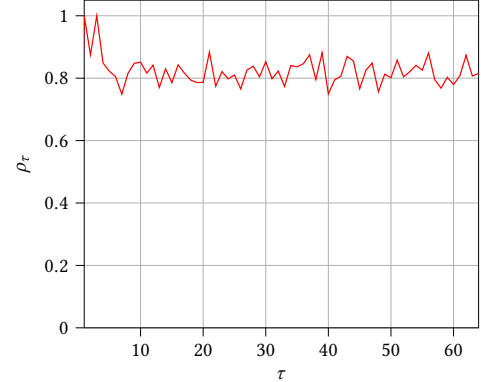


Figure 3: Maximum absolute correlation coefficients between $H_{\text{cw},\tau}$ and the power consumed by another parallel operating PE for different points in time τ . The results are generated by 10,000 simulations for random weight and input values.

the used implementation, already 2^{16} possible hypotheses must be evaluated if targeting the point where the register switches from the first intermediate result to the second. When assuming a manageable hypothesis space of 2^{64} , eight weights can be considered in the hypotheses at maximum, i.e., $\tau = 7$ is the last point where an attack is reasonable.

For a different number of used weights in the hypotheses, the average correlation between $H_{\text{cw},\tau}$ and the overall power consumption is determined empirically with Eq. (6) for uniform random weight and input values in Fig. 4. The course of the correlation coefficients is similar, independently of the targeted point in time τ . Moreover, the maximum correlation of the correct hypothesis $H_{\text{cw},\tau}$ is more significant compared to other hypotheses for a few parallel PEs. However, approximately at ten parallel operating PEs, the correlation coefficient of $H_{\text{cw},\tau=0}$ becomes smaller compared to others when targeting the first multiplication. If a later MAC operation is targeted, $H_{\text{cw},\tau}$ reaches this point at about 15 parallel PEs. Hence, Fig. 4 confirms a higher attack robustness if more MAC operations are used in the hypotheses.

The correlation reduction is limited in all cases and reaches its minimum for more than 30 parallel PEs. The correlation does not decrease further from this point on since the bit-width of the register limits the amount of possible power consumption values.

It is crucial to note that the statistical distribution of the weights does not impact the success of a CPA because it is independent of the actual values of the processed weights. Otherwise, it would not be possible to extract information through power consumption measurements. For example, in Appendix A, the results of a CPA are presented when the weights are normally distributed. In this case, the individual weight values tend to be more closely connected than when they are uniformly distributed. Nevertheless, the results in Appendix A are almost identical to those shown in Fig. 4, confirming the independence between a CPA and the actual values of the processed weights.

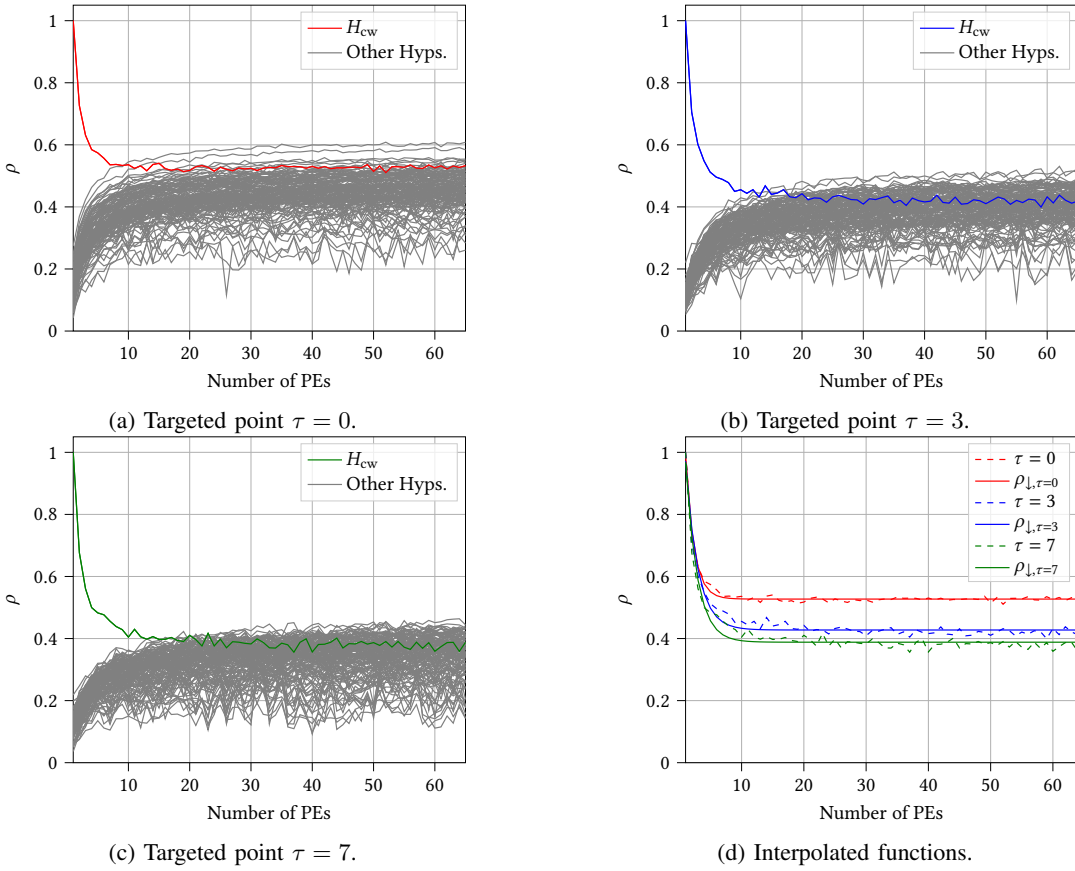


Figure 4: Absolute correlation coefficient for all possible hypotheses and an increasing number of parallel operating PEs. The results are averaged based on 10,000 simulations. The first multiplication is targeted in (a). For (b) and (c), the switching to the fourth or eighth MAC result is used. Interpolated functions that describe the decrease of the correlation coefficient for different τ are depicted in (d), where the results for the dashed lines are based on 10,000 simulation runs.

As the power consumption of different PEs is statistically dependent, it is not possible to simplify Eq. (6) to determine some equation that describes the behavior of the correlation coefficient for an increasing number of PEs. Nevertheless, Fig. 4 shows that the correct hypothesis's correlation decreases exponentially. Hence, the decrease $\rho_{\downarrow, \tau}$ for the correct hypothesis $H_{\text{cw}, \tau}$ based on the number of parallel PEs n_{PE} can be described as

$$\rho_{\downarrow, \tau}(n_{\text{PE}}) = a \cdot e^{(-b \cdot n_{\text{PE}})} + c. \quad (7)$$

The parameters a , b , and c must be determined based on the implementation and the targeted point in time τ . Here, exponential interpolation is used to determine the missing parameters of Eq. (7) based on the empirically calculated correlation values. The courses of the interpolations are depicted in Fig. 4d, where the dashed lines represent the results of $H_{\text{cw}, \tau}$ in Figs. 4a to 4c again for direct comparison. The interpolated functions for $\tau \in \{0, 3, 7\}$ are:

$$\rho_{\downarrow, \tau=0}(n_{\text{PE}}) = 0.369 \cdot e^{-0.637 \cdot n_{\text{PE}}} + 0.534, \quad (8)$$

$$\rho_{\downarrow, \tau=3}(n_{\text{PE}}) = 0.439 \cdot e^{-0.456 \cdot n_{\text{PE}}} + 0.431, \quad (9)$$

$$\rho_{\downarrow, \tau=7}(n_{\text{PE}}) = 0.482 \cdot e^{-0.507 \cdot n_{\text{PE}}} + 0.393. \quad (10)$$

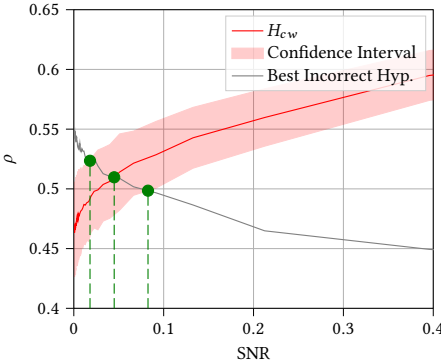
The maximum standard deviation between the listed functions and the simulated curves at a point n_{PE} does not exceed 0.0263. Further, interpolated equations for different τ can be found in Appendix B.

The theoretical findings can be used in other scenarios where the same input data is processed in parallel and a register stores the intermediate results within a PE, as no further implementation-specific assumptions are made.

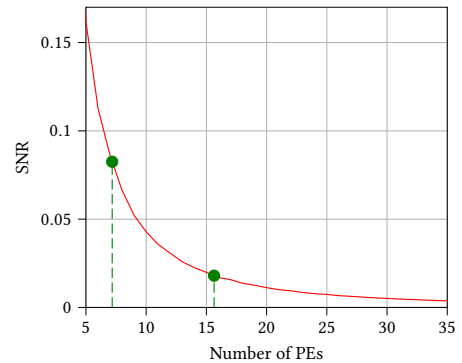
C. Success of Attack Based on the Signal-to-Noise Ratio

The results suggest that a CPA based on the overall power consumption of a vector-multiplication array becomes infeasible when 15 or more PEs operate in parallel. In such cases, the correlation of incorrect hypotheses exceeds that of the correct hypothesis. Therefore, AI accelerators that perform a small number of MAC operations simultaneously are already challenging to attack when an adversary relies on overall power consumption or global EM emissions.

To establish the success boundary for a CPA more broadly, the following analysis abstracts the number of implemented PEs in the vector-multiplication unit. In this context, the SNR is employed, which can be calculated independently of the



(a) Correlation depending on SNR.



(b) SNR based on implemented PEs.

Figure 5: In (a), the correlation coefficient for H_{cw} is shown as a function of the achieved SNR. The results are averaged based on 10,000 simulations. The confidence interval in (a) is calculated based on the targeted moments in time ranging from $\tau = 0$ to $\tau = 7$, while the solid red line indicates the mean value. The green points denote where the SNR is high enough to conduct a successful CPA. In (b), these points are also marked, indicating the SNR based on the number of PEs employed. These points correspond to the same number of PEs as described in Section III-B.

number of used PEs and the specific moment in time τ targeted. In Fig. 5a, the average correlation of the correct hypothesis H_{cw} , based on 10,000 simulations, is illustrated. The red area within the average curve of H_{cw} represents the behavior for $\tau \in \{0, 1, \dots, 7\}$.

The results indicate that, on average, an SNR of at least 0.045 is necessary for a successful attack. In the worst-case scenario, where either an early τ is selected for the attack or many PEs are implemented, achieving an SNR of at about 0.1 is essential to extract information about the weights of the NN. The region where the correlation of the correct hypothesis surpasses that of the best incorrect hypothesis indicates the previously used number of PEs. These points are also marked in Fig. 5b, which depicts the SNR as a function of the number of PEs. The crossing area shown in Fig. 5a is similarly highlighted in Fig. 5b, reflecting the range of PEs defined in Section III-B, up to which a CPA is successful.

Consequently, a general boundary based on the SNR is established, indicating that, on average, an SNR of at least 0.045 is required to enable successful weight retrieval. If the necessary SNR cannot be attained, localized EM measurements may be needed to enhance the SNR. Therefore, SCA targeting accelerators with more than 15 PEs necessitates local EM measurements using a probe capable of resolving no more than 15 PEs.

IV. EXPERIMENTAL RESULTS

This section provides practical results of how parallel computations within vector-multiplication units affect CPA, targeting extracting secret weight values. Different configurations of the PE array shown in Fig. 1 are used, which are realized on an FPGA. Consequently, various parallel operating resources are available, allowing the concurrent processing of neurons located within the same layer. The weight and input values are eight bits each, similar to the theoretical evaluation in Section III. The register that stores the intermediate results

within a PE has a bit-width of 32-bit. The results are based on a NewAE Technology CW305 Board that features a Xilinx Artix-7 FPGA, which operates at 1 MHz. The frequency of the FPGA is set to a low value for measurement purposes. At higher frequencies, the capacitors connected to the voltage supply line cause the power consumption to spread across consecutive clock cycles. This mixing of power consumption makes it difficult to retrieve accurate information, as data from multiple clock cycles become intertwined. However, the measurable operating frequency is highly dependent on the specific setup and devices used, i.e., different devices can operate at higher clock speeds based on the capacitive characteristics of the supply line.

While the FPGA is running, the power consumption is indirectly measured by a shunt resistor introduced in the voltage supply line. The signal of the shunt resistor is amplified by 20 dB through an on-chip amplifier. To collect the measurements, a PicoScope 6402D is used that samples at a frequency of 625 MHz. The processed weights are chosen randomly in the beginning and are the same across all measurements, i.e., the NN parameters remain constant. The inputs fed to the PE array are random and differ between consecutive measurements. To generate and flash the bitstreams, Vivado 2020.2 is used.

A. Correlation Power Analysis

An adversary can target different points in time τ to extract one or more secret weights processed by the vector-multiplication unit, as described in Section III. The targeted τ , however, affects the robustness of the attack depending on the achievable SNR as well as the computational complexity, as discussed in Sections III-B and III-C.

Initially, the focus is on the first multiplication of the PE array. The theoretical evaluation already shows that the first intermediate value provides less robust results when several PEs operate in parallel, compared to later points in time, as

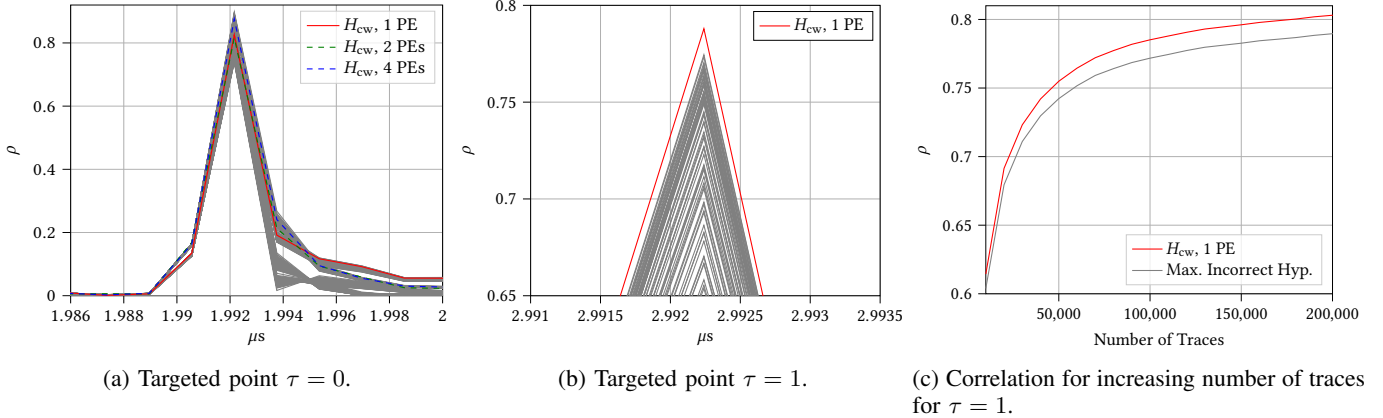


Figure 6: Absolute correlation between all hypotheses and 100,000 traces in (a) and (b), when targeting different points in time involving one or two weights in the hypotheses. The red curve represents the correct hypothesis if a single PE is implemented on the FPGA. The green and blue curves in (a) represent the correlation for the correct hypothesis when two or four PEs run in parallel, respectively. In (c), the correlation of $H_{\text{cw},\tau=1}$ is depicted across the number of traces used.

demonstrated by Fig. 4. Similar to the findings in Section III, the attacker concentrates on a single PE and tries extracting the weights processed here. Figure 6a shows the absolute correlation between all hypotheses and 100,000 measurements for a single implemented PE on the FPGA. The depicted time window represents the segment, where the first multiplication result between a weight and the corresponding input is stored in the register of the PE. The results show that the correct hypothesis does not achieve the maximum correlation. The reason is that when the result is stored in the register, the subsequent input is loaded, which is more dominant in the traces than switching the targeted register. For more parallel implemented PEs, this behavior is also the case, i.e., the correct hypothesis cannot be extracted due to the loading of the input, as shown by the dashed lines in Fig. 6a.

Consequently, it makes no sense to concentrate on the first multiplication at time $\tau = 0$, but the subsequent operation, i.e., the point where the register switches from the first intermediate result to the second. Here, the following input is still loaded, but the hypotheses no longer correlate with it, as the switching of the register is more accurately described by the used HD model. At the targeted point, 2^{16} hypotheses must be evaluated since two weights are attacked. The correct hypothesis's correlation coefficient is now higher than all others, as shown in Fig. 6b. Hence, it is possible to extract both weights $w_{\tau=0}$ and $w_{\tau=1}$ that are processed by the unit if a single PE is implemented, without any inaccuracies. Thereby, the attacker can maintain the strategy that always two weights (or even more) are attacked at once by choosing a later point in time τ . Alternatively, the adversary adapts the methodology by extracting one weight after the other to reduce computational complexity after the first two weights are recovered.

The simultaneous extraction of the first two weights demonstrates that the bit-width of the weights does not influence the success of a CPA. This can also be interpreted as an attack aimed at a single weight with a size of 16 bits.

To demonstrate that the amount of traces is sufficient, Fig. 6c shows how the correlation coefficient of $H_{\text{cw},\tau}$ changes when the number of traces increases. The results indicate that for the utilized FPGA, approximately 20,000 traces are sufficient to ensure that the correct hypothesis is larger than all other hypotheses.

The results show that CPA allows extracting information about the processed values if a single PE is implemented. In Fig. 7a, the maximum correlation of the correct hypothesis $H_{\text{cw},\tau}$ for an increasing number of PEs is depicted, again for time $\tau = 1$. Thereby, the same weights and random input values are used to ensure comparability for all experiments. The correct hypothesis $H_{\text{cw},\tau}$ reflects the weights that are processed by the same PE that is targeted in the case where just a single PE is implemented. However, if more than one PE is used, n_{PE} correct hypotheses exist. Therefore, in Fig. 7a, the highest correlation from one of the other correct hypotheses and the maximum correlation of all incorrect hypotheses are depicted. The results presented in Fig. 7a indicate that when more than eight PEs operate in parallel, none of the correct hypotheses attains the maximum correlation. From this point onward, incorrect hypotheses exhibit higher correlation coefficients. As shown in Section III-B, the theoretical results suggest that a CPA remains successful for up to 15 parallel operating PEs. The discrepancy between theoretical and practical results arises from the idealizations made in the theoretical analysis. Since noise components are not taken into account in the theoretical model, the CPA appears successful for a larger number of concurrently operating PEs. In contrast, the practical results inherently include noise and other physical effects that are not considered in Section III. Hence, from eight PEs onwards, it is impossible to extract any correct values from the FPGA implementation as the SNR is already below the boundary of about 0.02 and local EM measurements are needed that capture the emanations of four or fewer PEs.

The behavior shown in Fig. 7a is the same also for later

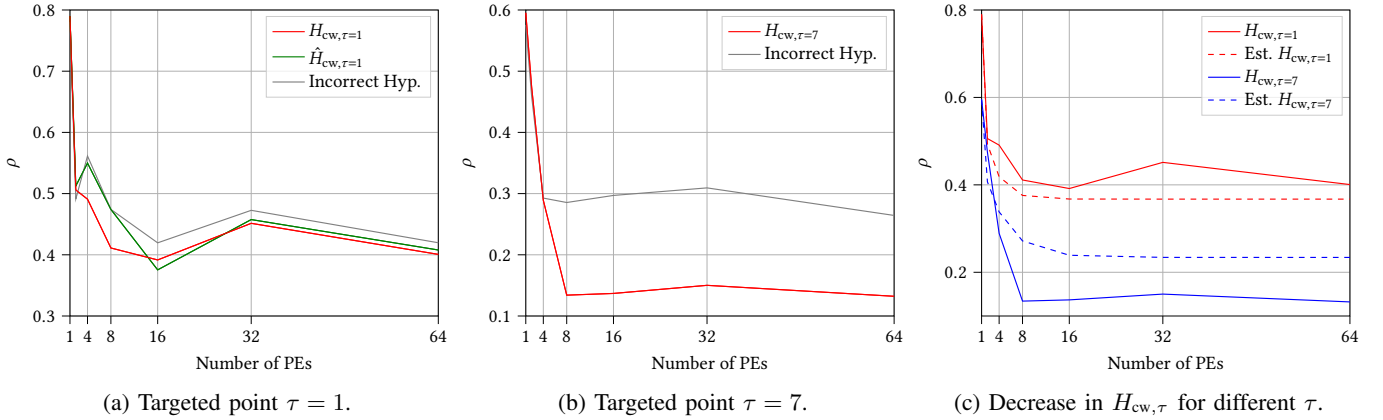


Figure 7: Absolute maximum correlation for an increasing number of parallel PEs at different τ is depicted in (a) and (b). The red curve represents the correct hypothesis $H_{cw,\tau}$, which is always processed by the first PE. More correct hypotheses exist for more than one implemented PE. The best candidate of all other correct hypotheses is represented by the green curve $\hat{H}_{cw,\tau}$ in (a). The gray curve depicts the maximum correlation of all wrong hypotheses. 100,000 traces are used with the same weights and inputs in all cases. The decrease in the correlation of $H_{cw,\tau}$ for different τ is shown in (c). Here, the solid lines represent the results from the measurements, while the dashed lines are calculated based on Eq. (7).

targeted points in time τ , although the theoretical results show a higher robustness if later τ are used, cf. Fig. 4. For instance, Fig. 7b demonstrates the results if $\tau = 7$ is used for the attack. In this case, not all possible hypotheses are calculated. Instead, the assumption is that the attacker already knows all weights processed by the targeted PE up to point $\tau = 6$. Hence, the attacker can calculate the intermediate result at $\tau = 6$ for the utilized inputs and uses the result to calculate the HD to the following intermediate result for all 256 weight hypotheses. However, as shown in Fig. 7b, the correct weight cannot be extracted for eight or more parallel operating PEs. Hence, the SNR is already too low in the case of a few parallel PEs to reliably extract values that are processed by the implementation on the FPGA. The findings match the current state of the art, where only small vector-multiplication units are targeted in the edge AI accelerator setting, cf. [7].

B. Influence of Parallelism on the Correlation Coefficient

This work demonstrates that the implementation of a PE array in a vector-multiplication unit that performs eight or more calculations in parallel is not attackable with CPA using the overall power consumption. However, one of the primary goals is to verify the correctness of Eq. (7) that describes the decrease in the correlation of the correct hypothesis $H_{cw,\tau}$, when the number of parallel PEs increases. For the evaluation, the focus is on $\tau = 1$ and $\tau = 7$, as these points in time are also used in Figs. 7a and 7b. In Fig. 7c, the correlation of $H_{cw,\tau}$ is shown when a varying number n_{PE} of PEs operate in parallel in the measurements. The dashed lines depict the theoretical course of $H_{cw,\tau}$ calculated based on Eq. (7). Figure 7c illustrates the estimated decrease of the correlation coefficient over the number of PEs for $\tau = 1$ and $\tau = 7$, as described by Eq. (7). The results confirm that the estimated curves derived from simulative results provide a

good approximation of the true course of the measured data. Consequently, Eq. (7) can be used to determine the decrease of the correlation for the correct hypothesis and confirms the findings in Section III.

As the weights of a trained NNs are not necessarily uniformly distributed, an additional evaluation is performed using the weight values from a trained layer of an NN. The results are similar to those shown in Fig. 7 and are detailed in Appendix C. Thus, the proposed findings are generic in their application and can be used to describe the behavior of a CPA targeting a vector-multiplication unit, independent of the actual values being processed.

Equation (7) cannot only be employed in the used setting. Besides edge AI accelerators, the findings can also be utilized in cases where the same input is processed in parallel with different secret data and stored in a register. The results may need little adaptation, but they generally remain valid. However, the findings of this paper are not amenable to cases like cryptographic implementations, where different inputs are processed simultaneously. The reason is that the inputs and, thus, the resulting power consumption portions are independent, cf. [25].

C. Discussion

The results of this work demonstrate that CPA attacks are only a serious threat to the confidentiality of parameters of NNs, which are executed on hardware accelerators with vector-multiplication units of low parallelism. In the case that an adversary targets the register where the intermediate results are stored, it is no longer possible to extract the correct value of a weight parameter if more than 15 weights are processed in parallel with the same input in the theoretical setting, without any noise, see Fig. 5. However, the practical results based on an FPGA show that with already eight parallel operating

PEs, none of the processed weights can be extracted when using the global power consumption. The poor performance on real hardware is due to other resources on the circuit and the measurement equipment itself, which all affect the quality of the measurements and decrease the SNR. This becomes evident when comparing idealized simulations to real-world measurements. While simulations yield a correlation coefficient of $\rho = 1$ for $n_{PE} = 1$ regardless of τ , the measured values are noticeably lower, e.g., $\rho_{n_{PE}=1,\tau=1} \approx 0.79$ and $\rho_{n_{PE}=1,\tau=7} \approx 0.6$. Moreover, the maximum incorrect hypotheses exhibit substantially higher correlation in practice (e.g., $\rho_{\text{Max,Incorrect},n_{PE}=1,\tau=1} \approx 0.77$ vs. ≈ 0.2 in simulations), further reducing the distinguishability between correct and incorrect hypotheses.

Nevertheless, the results indicate that parallel implementations of AI accelerators that are similar to the design used in this work, i.e., process several weights with the same input at a time and store the intermediate results in a register, lead to the same behavior when trying to reveal the weights by CPA. Consequently, CPA utilizing the overall power consumption is not a serious threat from a certain degree of parallelism. In the used case, the theoretical boundary is 15 parallel PEs or a SNR of about 0.02. Moreover, the state of the art indicates that other implementations behave similarly.

The analysis and results of this work demonstrate that for implementations that follow the leakage through the registers in PEs, no reliable information about the processed weights can be revealed through the overall power consumption if 15 or more PEs operate in parallel, from a theoretical point of view. Consequently, countermeasures must be reevaluated when only global power analysis attacks are considered threats, implying that the implementation follows similar leakage characteristics.

D. Impact on Other Designs and Countermeasures

Referring to existing AI accelerators that use a similar PE array as in this work, it is possible to make a statement about their vulnerability against power analysis attacks targeting the weight retrieval. The work of Bernardo et al. [23] uses a 8×8 PE array where one line of the array performs eight multiplications of the same input value with distinct weights. The theoretical findings of this work suggest that a CPA will be successful, since not more than 15 PEs operate in parallel processing the same input. However, the presented practical results show that already with eight concurrent PEs no information can be reliably extracted due to the noise, which is not considered in the theoretical part. Additionally, the design of Bernardo et al. introduces 56 other PEs that process different data and increase the noise in the power consumption, making a CPA more challenging.

Considering implementations like [21], [22], where the number of PEs can be adjusted during the design phase, the findings of this work establish a guideline for the optimal number of PEs to implement. The theoretical boundary of 15 parallel PEs minimizes the risk of a vulnerability to CPA that targets the weights.

To other designs with different data processing architectures, the findings of this paper may not be directly applicable. In this work, it is assumed that PEs process the same input data simultaneously, which may not be the case for systolic arrays, for example. The manner in which input data is combined with the neurons' weights is therefore critical in determining whether the results presented here can be applied to other architectures. For instance, in the publication of Adiono et al. [24], a small systolic array with nine PEs is utilized. The loading pattern is similar to the assumed pattern in this work, i.e., one input value is processed with nine distinct weights. Hence, the results of this work are amenable, and the theoretical findings indicate that the implementation of Adiono et al. is vulnerable to attacks like CPA utilizing the device's power consumption. However, the practical analysis of the FPGA in Section IV-A demonstrates that the implementation is likely to be challenging to attack, when implemented on a real device. This is due to the use of more than eight PEs and the presence of noise in the actual measurements, which reduces the SNR and consequently lowers the probability of success.

In contrast, the analyzed 3×3 systolic array by Yoshida et al. [7] processes one weight or several distinct weights with different input values. As the PEs in the array process different inputs, their power consumption is independent of the power consumed by the targeted PE. Hence, the statistical independent noise is more significant in the work of [7] that the authors reduce by performing several CPAs sequentially, allowing successful weight extraction. However, the findings of Yoshida et al. are in line with this work since the practical analysis shows that with up to eight PEs processing the same input value at a time, a CPA allows reliable extraction of the weights.

Furthermore, the presented analysis is already described little by the work of Gongye et al. [8]. They show that a CPA targeting weight extraction on a highly parallel hardware accelerator is only possible for kernels used in CNNs, when all inputs except one are set to zero. Otherwise, not only one kernel weight is processed, making the attack no longer possible. The authors mention that with local EM measurements, an attack may be possible if a single PEs can be located. However, no theoretical or practical analysis of the effects of concurrent operating PEs on power consumption and the success of a CPA is performed in [8]. The results of this work align with the findings of [8] and provide a more theoretical analysis of how CPA behaves for vector-multiplications with different degrees of parallelism.

Considering countermeasures against CPA, masking is a well-known technique to hinder power analysis attacks. By introducing random numbers into the calculations during the inference of an NN, masking breaks the dependency between processed data and power consumption. Attacks like CPA are no longer possible since an adversary cannot generate correct hypotheses based on the input values, as the random numbers are unknown. The acquired traces must be pre-processed to enable a so-called higher-order attack, which is more complex and often no longer practically possible. In particular, no

higher-order attack is known for NN implementations at the time of this paper's publication.

Masking is commonly used in the context of NNs to protect the secret weights, which are processed by PEs [14], [17], [26]. As masked implementations are typically proven formally secure, no information is leaked through a side-channel up to a certain order. With respect to the results of this paper, masked implementations are beneficial for NN implementations with low parallelism, i.e., a vector-multiplication unit with less than 15 PEs, when considering the theoretical boundary. For designs with a higher degree of parallelism where the same input value is processed at a time, masking is not necessary, as from a theoretical point of view, no weights can be extracted via the overall power consumption. If local EM-based attacks are also an assumed threat, masking is a possible extension to prohibit attacks in this scenario.

However, masking is commonly an expensive countermeasure that requires significant modifications of the calculations and the hardware itself [17]. Furthermore, a large amount of random numbers is required, which are an expensive resource. Shuffling is a potentially easier-to-implement countermeasure requiring less randomness [15]. Shuffling randomizes the execution order of neurons of a layer and the multiplications performed within a neuron. Hence, it is no longer known which neuron and which weight of a neuron is executed. As a result, the acquired traces are no longer aligned, i.e., distinct operations are performed at a defined moment, leading to a decrease in the SNR. Therefore, the effort in terms of measurements increases quadratically, which already makes an attack on a small NN with tens of neurons challenging [15]. A prerequisite for shuffling is that not all neurons of a layer can be executed entirely in parallel. Consequently, shuffling is well-suited for small accelerators that perform fewer than 15 calculations concurrently to enhance the protection against power analysis attacks. The used vector-multiplication unit utilizes the same input value for all PEs, similar to implementations like [21]–[23]. Thus, the parallel operating neurons cannot process distinct input values, limiting the maximum amount of theoretically possible shuffling opportunities. However, overall, shuffling enhances the protection against CPA and also local EM-based attacks since even if an adversary can resolve a single PE, the traces are not aligned.

In conclusion, masking and shuffling are well-suited for small accelerators that perform fewer than 15 calculations in parallel. While shuffling is less expensive and easier to implement, masking provides provable security, which may be necessary in critical sectors. For accelerators that perform more than 15 multiplications with distinct weights in parallel, additional countermeasures make sense if protection against more advanced attacks is required, like local EM attacks. However this work suggests, that for simultaneously operating PEs, the inherent noise from concurrent operations naturally limits exploitable information, enhancing resistance to power consumption based side-channel attacks. Thus, parallel execution of neurons not only improves computational throughput but also provides an intrinsic security benefit.

V. CONCLUSION

The current state of the art indicates that a CPA targeting the MAC operations of parallel AI accelerators has limited success using power consumption. For a reliable attack, local EM measurements are necessary. However, no comprehensive analysis has been conducted up to now that examines the effects of concurrent calculations on power consumption, nor has any research determined the point at which the SNR becomes too low to exploit secret information.

This work evaluates in detail the influence of parallelism within AI accelerators on CPA, which targets extracting secret weight values. As vector-multiplication units process the same input with different weights in parallel, the influence is different in the described setting compared to cryptographic implementations. The parallel processing of the same input is why the power consumption of the individual operations is not statistically independent of each other. This impacts the correlation of the correct weight hypothesis with an increasing number of parallel PEs, as shown by the theoretical analysis. When 15 or more PEs process data concurrently, reliable weight extraction is no longer possible. Depending on the attack's point in time, equations that describe the decrease in the correlation coefficient for the correct weight hypothesis in dependence on the degree of parallelism are deduced. The correctness of the equations is demonstrated by practical measurement data acquired from an FPGA implementation. In contrast to the idealized theoretical results, the real-world traces allow no successful weight retrieval with already eight parallel PEs. The lower boundary is due to the additional noise not considered in the theoretical setting. However, the equations allow to estimate the behavior of the correlation coefficient depending on the number of parallel operations. Thereby, it is possible to determine the degree of parallelism from which on CPA, utilizing the overall power consumption is no longer a serious threat, and local EM measurements are required to reliably extract information.

The effects on CPA differ when the PE array processes dissimilar input data simultaneously. For statistically independent input values, the correlation of the correct hypothesis follows the behavior described by Mangard et al. [25]. As the proportion of distinct inputs increases, the noise component in the power consumption also rises, leading to a decrease in the SNR. This reduction in SNR can be mitigated by increasing the number of measurements, thereby enabling a successful CPA. When the PE array processes a combination of identical and distinct input values in parallel, the resulting intermediate values comprise both statistically dependent and independent components. Such scenarios offer a promising direction for further investigation to fully characterize the impact of mixed input processing on CPA.

REFERENCES

- [1] S. Han, H. Mao, and W. J. Dally, "Deep compression: Compressing deep neural networks with pruning, trained quantization and huffman coding," *arXiv preprint arXiv:1510.00149*, 2015.

[2] B. Jacob, S. Kligys, B. Chen, M. Zhu, M. Tang, A. Howard, H. Adam, and D. Kalenichenko, "Quantization and training of neural networks for efficient integer-arithmetic-only inference," in *Proceedings of the IEEE Conference on Computer Vision and Pattern Recognition*, pp. 2704–2713, 2018.

[3] L. Deng, G. Li, S. Han, L. Shi, and Y. Xie, "Model compression and hardware acceleration for neural networks: A comprehensive survey," *Proceedings of the IEEE*, vol. 108, no. 4, pp. 485–532, 2020.

[4] S. Han, X. Liu, H. Mao, J. Pu, A. Pedram, M. A. Horowitz, and W. J. Dally, "Eie: efficient inference engine on compressed deep neural network," *ACM SIGARCH Computer Architecture News*, vol. 44, no. 3, pp. 243–254, 2016.

[5] E. Brier, C. Clavier, and F. Olivier, "Correlation power analysis with a leakage model," in *International workshop on cryptographic hardware and embedded systems*, pp. 16–29, Springer, 2004.

[6] L. Batina, S. Bhasin, D. Jap, and S. Picek, "Poster: Recovering the input of neural networks via single shot side-channel attacks," in *Proceedings of the 2019 ACM SIGSAC Conference on Computer and Communications Security*, pp. 2657–2659, 2019.

[7] K. Yoshida, T. Kubota, S. Okura, M. Shiozaki, and T. Fujino, "Model reverse-engineering attack using correlation power analysis against systolic array based neural network accelerator," in *2020 IEEE International Symposium on Circuits and Systems (ISCAS)*, pp. 1–5, IEEE, 2020.

[8] C. Gongye, Y. Luo, X. Xu, and Y. Fei, "Side-channel-assisted reverse-engineering of encrypted dns hardware accelerator ip and attack surface exploration," in *2024 IEEE Symposium on Security and Privacy (SP)*, pp. 4678–4695, IEEE, May 2024.

[9] G. Takatoi, T. Sugawara, K. Sakiyama, and Y. Li, "Simple electromagnetic analysis against activation functions of deep neural networks," *tech. rep.*, 2020.

[10] S. Maji, U. Banerjee, and A. P. Chandrakasan, "Leaky nets: Recovering embedded neural network models and inputs through simple power and timing side-channels—attacks and defenses," *IEEE Internet of Things Journal*, vol. 8, pp. 12079–12092, Aug. 2021.

[11] H. Yu, H. Ma, K. Yang, Y. Zhao, and Y. Jin, "Deepem: Deep neural networks model recovery through em side-channel information leakage," in *2020 IEEE International Symposium on Hardware Oriented Security and Trust (HOST)*, pp. 209–218, IEEE, Dec. 2020.

[12] L. Batina, S. Bhasin, D. Jap, and S. Picek, "{CSI}{NN}: Reverse engineering of neural network architectures through electromagnetic side channel," in *28th {USENIX} Security Symposium ({USENIX} Security 19)*, pp. 515–532, 2019.

[13] I. N. Da Silva, D. H. Spatti, R. A. Flauzino, L. H. B. Liboni, and S. F. dos Reis Alves, "Artificial neural network architectures and training processes," in *Artificial neural networks*, pp. 21–28, Springer, 2017.

[14] A. Dubey, A. Ahmad, M. A. Pasha, R. Cammarota, and A. Aysu, "ModuloNET: Neural networks meet modular arithmetic for efficient hardware masking," *IACR Transactions on Cryptographic Hardware and Embedded Systems*, pp. 506–556, nov 2021.

[15] M. Brosch, M. Probst, and G. Sigl, "Counteract side-channel analysis of neural networks by shuffling," in *2022 Design, Automation & Test in Europe Conference & Exhibition (DATE)*, (Antwerp, Belgium), IEEE, Mar 2022.

[16] K. Athanasiou, T. Wahl, A. A. Ding, and Y. Fei, "Masking feedforward neural networks against power analysis attacks," *Proceedings on Privacy Enhancing Technologies*, vol. 2022, no. 1, pp. 501–521, 2022.

[17] M. Brosch, M. Probst, M. Glaser, and G. Sigl, "A masked hardware accelerator for feed-forward neural networks with fixed-point arithmetic," *IEEE Transactions on Very Large Scale Integration (VLSI) Systems*, 2023.

[18] M. Probst, M. Brosch, and G. Sigl, "Side-channel analysis of integrate-and-fire neurons within spiking neural networks," *IEEE Transactions on Circuits and Systems I: Regular Papers*, pp. 1–13, 2024.

[19] A. Bagheri, O. Simeone, and B. Rajendran, "Adversarial training for probabilistic spiking neural networks," in *2018 IEEE 19th International Workshop on Signal Processing Advances in Wireless Communications (SPAWC)*, pp. 1–5, IEEE, 2018.

[20] M. Fredrikson, E. Lantz, S. Jha, S. Lin, D. Page, and T. Ristenpart, "Privacy in pharmacogenetics: An {End-to-End} case study of personalized warfarin dosing," in *23rd USENIX Security Symposium (USENIX Security 14)*, pp. 17–32, 2014.

[21] S. Yin, S. Tang, X. Lin, P. Ouyang, F. Tu, L. Liu, and S. Wei, "A high throughput acceleration for hybrid neural networks with efficient resource management on fpga," *IEEE Transactions on Computer-Aided Design of Integrated Circuits and Systems*, vol. 38, pp. 678–691, Apr. 2019.

[22] C. Zhang, G. Sun, Z. Fang, P. Zhou, and J. Cong, "Caffeine: Towards uniformed representation and acceleration for deep convolutional neural networks," in *Proceedings of the ACM Turing Award Celebration Conference - China 2023*, ACM TURC '23, pp. 47–48, ACM, July 2023.

[23] P. P. Bernardo, C. Gerum, A. Frischknecht, K. Lubeck, and O. Bringmann, "Ultratrail: A configurable ultralow-power tc-resnet ai accelerator for efficient keyword spotting," *IEEE Transactions on Computer-Aided Design of Integrated Circuits and Systems*, vol. 39, pp. 4240–4251, Nov. 2020.

[24] T. Adiono, G. Meliolla, E. Setiawan, and S. Harimurti, "Design of neural network architecture using systolic array implemented in verilog code," in *2018 International Symposium on Electronics and Smart Devices (ISESD)*, pp. 1–4, IEEE, Oct. 2018.

[25] S. Mangard, E. Oswald, and T. Popp, *Power analysis attacks: Revealing the secrets of smart cards*, vol. 31. Springer Science & Business Media, 2008.

[26] S. Maji, U. Banerjee, S. H. Fuller, and A. P. Chandrakasan, "A threshold implementation-based neural network accelerator with power and electromagnetic side-channel countermeasures," *IEEE Journal of Solid-State Circuits*, vol. 58, pp. 141–154, jan 2023.

APPENDIX

A. Correlation Power Analysis with Normally Distributed Weights

In the following, for a varying number of used weights in the hypotheses, the average correlation between $H_{\text{cw},\tau}$ and the overall power consumption is determined empirically with Eq. (6) for normally randomly distributed weights with a standard deviation of $\sigma = 20$. The course of the correlation coefficients is similar to the results depicted in Fig. 4, demonstrating the independence between the CPA and the actual values of the processed weights.

B. Interpolated Functions

In the following, the values for the first eight interpolated functions are provided that describe the decrease of the correlation coefficient ρ_{\downarrow} for the correct weight hypothesis $H_{\text{cw},\tau}$. Furthermore, the maximum standard deviation σ for each equation is provided.

$$\begin{aligned} \rho_{\downarrow,\tau=0}(n_{\text{PE}}) &= 0.369 \cdot e^{-0.637 \cdot n_{\text{PE}}} + 0.534, & \sigma \approx 0.011762 \\ \rho_{\downarrow,\tau=1}(n_{\text{PE}}) &= 0.392 \cdot e^{-0.450 \cdot n_{\text{PE}}} + 0.465, & \sigma \approx 0.029043 \\ \rho_{\downarrow,\tau=3}(n_{\text{PE}}) &= 0.439 \cdot e^{-0.456 \cdot n_{\text{PE}}} + 0.431, & \sigma \approx 0.024154 \\ \rho_{\downarrow,\tau=2}(n_{\text{PE}}) &= 0.441 \cdot e^{-0.532 \cdot n_{\text{PE}}} + 0.449, & \sigma \approx 0.022669 \\ \rho_{\downarrow,\tau=4}(n_{\text{PE}}) &= 0.468 \cdot e^{-0.473 \cdot n_{\text{PE}}} + 0.419, & \sigma \approx 0.022269 \\ \rho_{\downarrow,\tau=5}(n_{\text{PE}}) &= 0.494 \cdot e^{-0.511 \cdot n_{\text{PE}}} + 0.413, & \sigma \approx 0.019673 \\ \rho_{\downarrow,\tau=6}(n_{\text{PE}}) &= 0.457 \cdot e^{-0.470 \cdot n_{\text{PE}}} + 0.407, & \sigma \approx 0.026922 \\ \rho_{\downarrow,\tau=7}(n_{\text{PE}}) &= 0.482 \cdot e^{-0.507 \cdot n_{\text{PE}}} + 0.393, & \sigma \approx 0.026230. \end{aligned}$$

C. Correlation Power Analysis Targeting Trained Weights

Figure 9 displays the results when targeting the FPGA processing a trained fully-connected layer. The weights are from the first layer of an MLP trained with the MNIST dataset of handwritten numbers. The results, are similar to those discussed in Section IV-A.

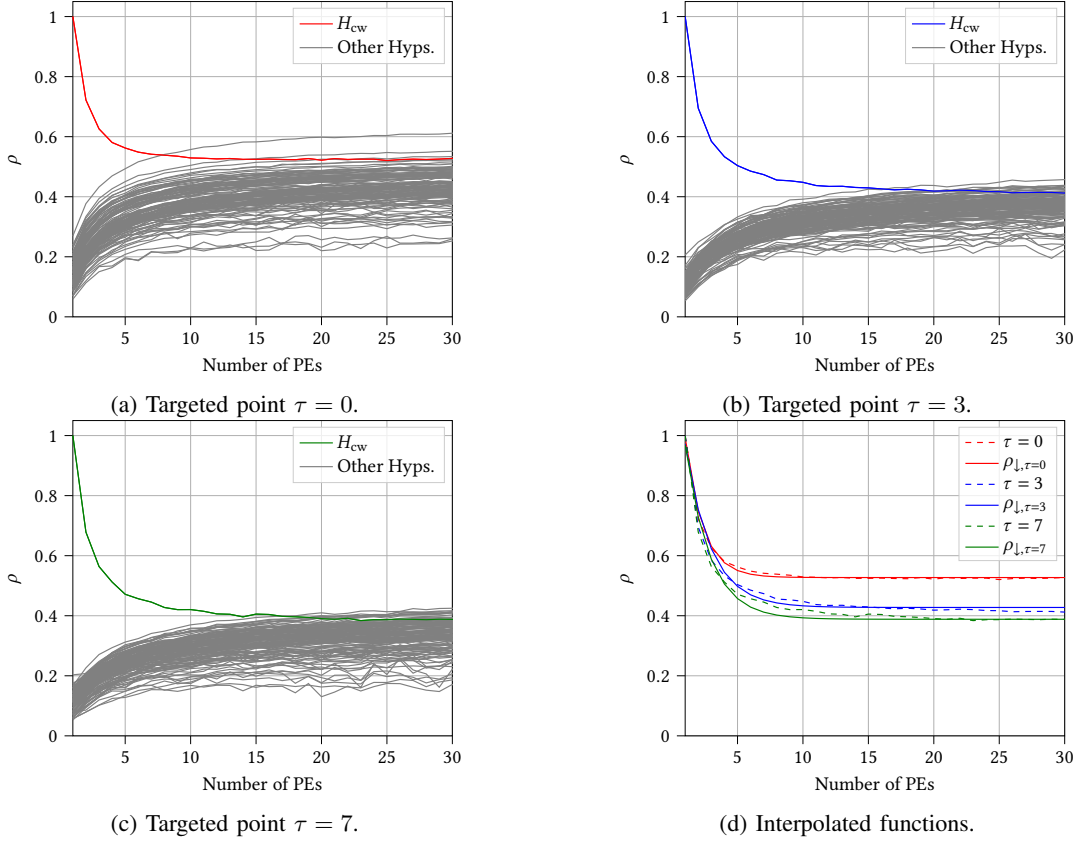


Figure 8: Absolute correlation coefficient for all possible hypotheses and an increasing number of parallel operating PEs. The results are based on 10,000 simulations. The first multiplication is targeted in (a). For (b) and (c), the switching to the fourth or eighth MAC result is used. In (d) the results of (a) to (c) are depicted again together with the interpolated functions based on the listed equations in Section B, which demonstrates that the interpolations are also amenable to other distributions.

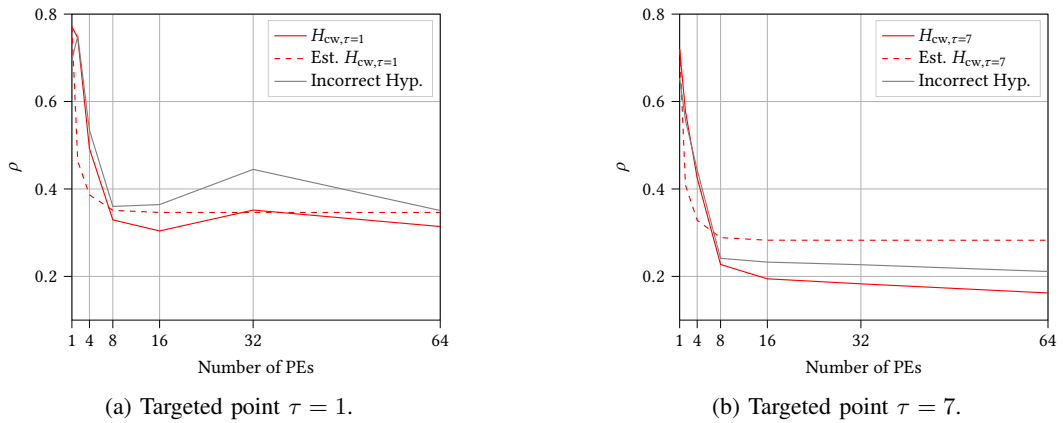


Figure 9: Absolute maximum correlation for an increasing number of parallel PEs at different τ is depicted in (a) and (b). The red curve represents the correct hypothesis $H_{cw,\tau}$, which is always processed by the first PE. The gray curve depicts the maximum correlation of all wrong hypotheses. The decrease in the correlation of $H_{cw,\tau}$ for the respective τ is shown by the dashed lines. 100,000 traces are used in all cases.